

25. THE ROLES OF CLIMATE CHANGE AND EL NIÑO IN THE RECORD LOW RAINFALL IN OCTOBER 2015 IN TASMANIA, AUSTRALIA

DAVID J. KAROLY, MITCHELL T. BLACK, MICHAEL R. GROSE, AND ANDREW D. KING

Anthropogenic climate change and El Niño made small but significant contributions to increasing the likelihood of record low rainfall in October 2015 in Tasmania. Atmospheric variability was the main contributor.

Introduction. The island state of Tasmania, in southeast Australia, received record low average rainfall of 21 mm in October 2015, 17% of the 1961–90 normal (Fig. 25.1a; Bureau of Meteorology 2015). This had major impacts across the state, affecting agriculture and hydroelectric power generation and preconditioning the landscape for major bushfires the following summer (Hobday et al. 2016). Rainfall in Tasmania is normally high throughout the year, with variations in Austral spring associated with mean sea level pressure (MSLP) and circulation variations due to El Niño, the Indian Ocean dipole (IOD), and the southern annular mode (SAM; Hill et al. 2009). Spring rainfall is declining and projected to decrease further in Tasmania (Hope et al. 2015)

This record low rainfall was associated with extreme high MSLP over much of southeast Australia (Fig. 25.1b) and record high October mean maximum temperature over southern Australia (Black and Karoly 2016). The wave train pattern of MSLP anomalies in October (Fig. 25.1b) from southern Australia across the South Pacific is typical of the Pacific South American (PSA) pattern (Mo and Higgins 1998). El Niño conditions, such as in late 2015, are associated with a shift in tropical Pacific rainfall and in waveguides in the extratropical Pacific that influence the PSA pattern (Karoly 1989) and rainfall in Tasmania.

We have investigated the roles of anthropogenic climate change, the 2015/16 El Niño, and internal

atmospheric variability on this record low October rainfall using observational data, regional climate simulations driven by specified sea surface temperatures (SSTs) from the weather@home Australia and New Zealand (w@h ANZ) project (Black et al. 2015, 2016; Massey et al. 2015), and coupled climate model simulations from the Coupled

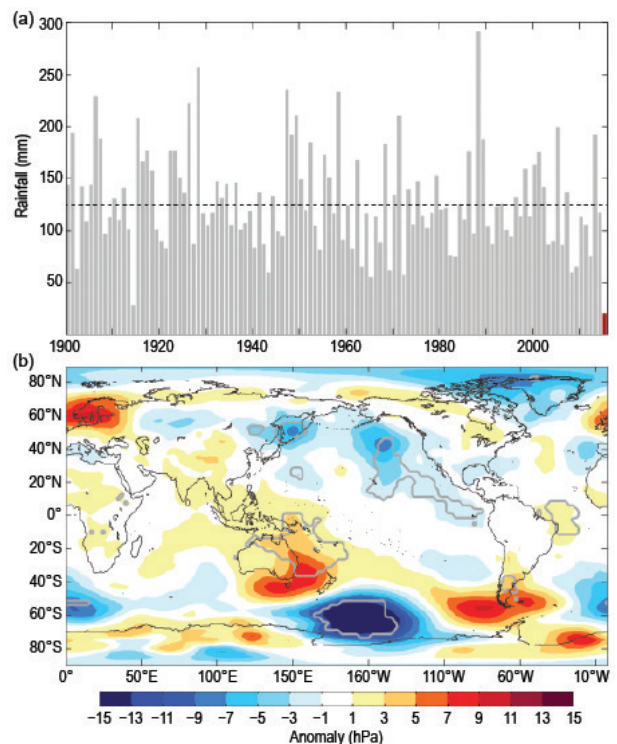


FIG. 25.1. (a) Observed Oct mean rainfall (mm) for Tasmania for 1900–2015 from the Australian Bureau of Meteorology, with 2015 highlighted in red. The dashed line shows the 1900–2015 average. (b) Mean sea level pressure anomalies (MSLP, hPa) for Oct 2015 from NCEP–NCAR reanalyses (Kalnay et al. 1996). Regions with record high and low Oct MSLP values in the reanalyses are outlined by gray lines.

AFFILIATIONS: KAROLY, BLACK, AND KING—School of Earth Sciences and ARC Centre of Excellence for Climate System Science, University of Melbourne, Victoria, Australia; GROSE—CSIRO Climate Science Centre, Hobart, Tasmania, Australia
DOI:10.1175/BAMS-D-16-0139.1

A supplement to this article is available online (10.1175/BAMS-D-16-0139.2)

Model Intercomparison Project phase 5 (CMIP5; Taylor et al. 2012).

Data and Methods. Monthly area-average rainfall data for Tasmania were obtained from the Australian Bureau of Meteorology. The October rainfall for 1900–2015 was obtained from high-resolution gridded data from the Australian Water Availability Project (AWAP; Jones et al. 2009). The dataset uses all available monthly rainfall station data, with sparser station coverage early in the period.

Very large ensembles of regional climate simulations of rainfall over Tasmania were used from the w@h ANZ project. This uses the atmosphere-only model, HadAM3P, to drive a nested regional model (HadRM3P; 0.44° resolution). For details of the modeling setup, see Black et al. (2016). First, the model was run under two climate scenarios for 2015: observed (all forcings; ALL) and counterfactual (natural forcings only; NAT) realizations. For the ALL simulations, the model used observed SSTs and sea ice from the Operational Sea Surface Temperature and Sea Ice Analysis (OSTIA; Donlon et al. 2012), as well as present-day atmospheric composition (long-lived greenhouse gases, ozone, and aerosols). Very large ensembles were generated by running the model with perturbed atmospheric initial conditions. For the NAT simulations, the model was driven by preindustrial atmospheric composition and SSTs modified to remove different estimates of the warming attributable to anthropogenic forcing. Estimates of the SST changes due to anthropogenic forcing were separately calculated using eight CMIP5 models (Taylor et al. 2012; see online Supplemental Material), giving eight realizations of possible NAT SSTs. The main modes of natural variability represented in the ALL SSTs (e.g., the phase of El Niño) are maintained in the NAT SSTs. Therefore, any change in likelihood of low Tasmanian rainfall between these ALL and NAT scenarios can be directly attributed to anthropogenic forcing (Black et al. 2015).

To assess the influence of El Niño on Tasmanian rainfall, additional simulations were generated by driving the w@h ANZ model with composite SST patterns representative of El Niño, Neutral, and La Niña phases (see supplemental material). Each of these three phases was modeled under both ALL and NAT climate scenarios (as for the 2015 runs). Previous analysis has shown that the w@h ANZ model is able to represent El Niño teleconnections over Australia (Black et al. 2016).

We used all the model simulations that were available; more than 2700 members for each of the ALL scenarios (2015 ALL, El Niño ALL, Neutral ALL, and La Niña ALL) and more than 650 members for each of the corresponding eight NAT realizations (at least 5200 members for each NAT scenario).

Following Black et al. (2016), we corrected any model rainfall bias by scaling the Tasmanian October rainfall from the ALL simulations so that the mean of the distribution is equal to that of the recent AWAP observations (1985–2014). This bias adjustment is then applied to the NAT distribution.

To examine possible changes in the likelihood of extreme low October rainfall, we define a threshold based on the previous observed record (56 mm in 1965; see Fig. 25.1a) rather than the 2015 record, to reduce selection bias. The 1914 low rainfall value was not used because of the smaller number of rainfall stations available then, which limits the reliability of the Tasmanian rainfall estimate given the varied topography across the state. The current rainfall station network across Tasmania has been relatively stable since the mid-1950s.

To quantify the change in likelihood of extreme low rainfall due to different forcing scenarios, we calculate the fraction of attributable risk (FAR; Allen 2003), defined as $FAR = 1 - (P_1 / P_2)$. We estimate the anthropogenic (El Niño) influence by setting P_1 to be the probability of rainfall lower than the October threshold in the NAT (La Niña and Neutral) simulations, while P_2 is the equivalent for the ALL (El Niño) simulations. Hence, we are able to quantify the change in likelihood due to either anthropogenic forcing or El Niño. FAR uncertainty was estimated by bootstrap resampling groups of 1000 simulations from each of the ensembles (10 000 times with replacement) and the 10th percentile FAR value is used to provide conservative estimates of changes in likelihood associated with the different forcing.

Coupled climate model data were extracted from the CMIP5 archive and evaluated for their performance in capturing observed variability of Tasmanian rainfall. The model data were regridded onto a 2° grid and October rainfall over Tasmania and July–December Niño-3.4 SST values were extracted. Simulations from the “historical” experiment (including natural and anthropogenic forcings for 1861–2005) were compared with observations over 1951–2005. Models with at least three historical simulations were tested for similarity to observational data following King et al. (2016). The twelve models

that passed this evaluation are listed in supplemental material. Given the coarse model resolution and poor representation of topography in western Tasmania, the simulated rainfall anomalies were assessed as percentage anomalies from the 1961–90 historical average, removing any rainfall bias.

October rainfall and Niño-3.4 data were extracted from the historicalNat (natural forcings only for 1861–2005) simulations and RCP8.5 (projected climate under a high greenhouse gas emissions scenario for 2006–35) simulations. The historical and matching RCP8.5 simulations were combined to provide an ALL forcing ensemble for 1995–2035 (40 years centered on 2015), which was compared with the NAT ensemble (1861–2005) using the historicalNat runs. These ensembles were then used to investigate the change in likelihood of low rainfall due to anthropogenic climate change.

Results. The observed October rainfall data show a significant but small correlation with El Niño and a small, nonsignificant drying trend. The linear regression estimate of the October 2015 rainfall anomaly associated with the Niño-3.4 SST value is -26 ± 10 mm.

Assessment of the probability distributions of October rainfall from the w@h ANZ simulations (Fig. 25.2a) shows good agreement with observations and that the ALL ensembles are significantly drier than the NAT ensembles for both the 2015 and composite El Niño scenarios. The drying is about 8 mm for the median and about 5 mm for the 5th percentile. A mean drying of about 6% is also found in the CMIP5 simulations (Fig. 25.2a).

The October rainfall distribution from the w@h ANZ El Niño ALL ensemble is also drier than the combined Neutral/La Niña ensemble (Fig. 25.2a), with a drying of about 5 mm for the 5th percentile. This is much smaller than the observational-estimated anomaly for the 2015 El Niño. This El Niño analysis was not undertaken for the CMIP5 simulations due to the smaller number of El Niño years available.

Next, the change in likelihood of record low rainfall below the 1965 threshold is assessed for the different scenarios, using the FAR results shown in Fig. 25.2b. For the w@h ANZ simulations, anthropogenic forcing *very likely* increases the likelihood of low rainfall by at least 39% (median increase 75%) for the 2015 scenario and by at least 18% (median increase 59%) for the composite El Niño scenario. For the CMIP5 simulations, the FAR results

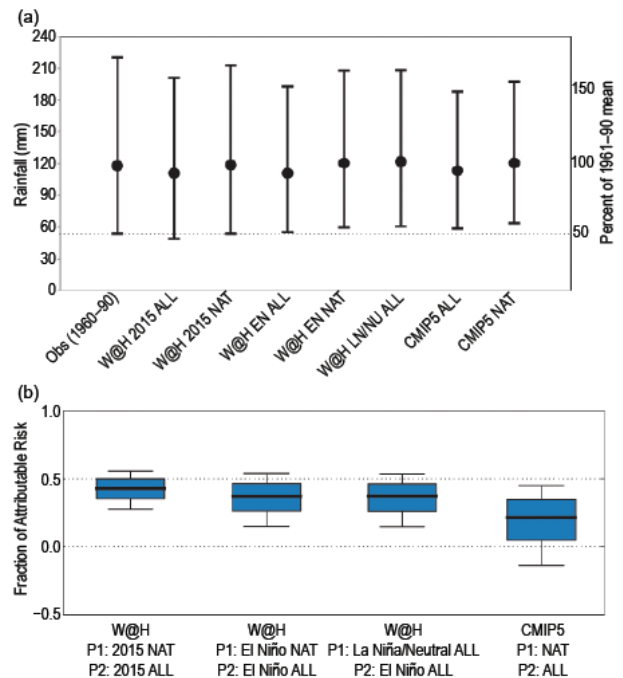


FIG. 25.2. (a) Distributions of Oct mean rainfall rate for Tasmania for the various model scenarios. Each vertical line spans the range from the 5th percentile to the 95th percentile, with the median marked. The dotted line is the Oct 1965 observed rainfall. (b) Corresponding distributions of FAR for rainfall below the 1965 threshold for the different scenario combinations for P1 and P2. Boxes show the median and interquartile range while whiskers extend to the 10th and 90th percentiles.

are less certain, with anthropogenic forcing possibly decreasing the likelihood by 12% or increasing it by up to 82%, with a median increase of 25%. Using the w@h ANZ simulations again, El Niño very likely increases the risk of low October rainfall by at least 18% (median increase 59%).

There are circulation differences between the w@h ANZ ALL and NAT simulations that are consistent with the response to anthropogenic forcing, including higher MSLP in middle latitudes and a significantly more positive SAM index in the ALL scenario, as found also in the CMIP5 simulations (Gillett et al. 2013).

Conclusions. Tasmania experienced its driest October on record in 2015. Anthropogenic climate change and the strong El Niño in 2015 *very likely* increased the chances of breaking the previous record low rainfall in 1965. In terms of contributions to the magnitude of this rainfall deficit, internal atmospheric variability as indicated by the PSA MSLP pattern (Fig. 25.1b)

was likely the main contributor, with El Niño next and a smaller but significant contribution from anthropogenic climate change.

ACKNOWLEDGEMENTS. This research was supported by the ARC Centre of Excellence for Climate System Science (grant CE 110001028) and the National Environmental Science Programme Earth Systems and Climate Change Hub. In addition, weather@home ANZ involves collaboration with Oxford University, the Met Office, NIWA in New Zealand, and the Tasmanian Partnership for Advanced Computing. We acknowledge the WCRP Working Group on Coupled Modelling, which is responsible for CMIP5 and thank the climate modeling groups for making available their model output.

REFERENCES

- Allen, M., 2003: Liability for climate change. *Nature*, **421**, 891–892.
- Black, M. T., and D. J. Karoly, 2016: Southern Australia's warmest October on record: The role of ENSO and climate change [in "Explaining Extreme Events of 2015 from a Climate Perspective"]. *Bull. Amer. Meteor. Soc.*, **97** (12), S118–S121, doi:10.1175/BAMS-D-16-0124.1. (chapter 20 of EEE)
- Black, M. T., D. J. Karoly, and A. D. King, 2015: The contribution of anthropogenic forcing to the Adelaide and Melbourne, Australia, heat waves of January 2014 [in "Explaining Extreme Events of 2014 from a Climate Perspective"]. *Bull. Amer. Meteor. Soc.*, **96** (12), S145–S148, doi:10.1175/BAMS-D-15-00097.1.
- , —, and Coauthors, 2016: The weather@home regional climate modelling project for Australia and New Zealand. *Geosci. Model Dev.*, **9**, 3161–3176, doi:10.5194/gmd-9-3161-2016.
- Bureau of Meteorology, 2015: Special Climate Statement 52: Australia's warmest October on record, version 2.1, updated 2 Dec 2015. Bureau of Meteorology, 25 pp. [Available online at www.bom.gov.au/climate/current/statements/scs52.pdf.]
- Donlon, C. J., M. Martin, J. Stark, J. Roberts-Jones, E. Fiedler, and W. Wimmer, 2012: The Operational Sea Surface Temperature and Sea Ice Analysis (OSTIA) system. *Remote Sens. Environ.*, **116**, 140–158, doi:10.1016/j.rse.2010.10.017.
- Gillett, N. P., J. C. Fyfe, and D. E. Parker, 2013: Attribution of observed sea level pressure trends to greenhouse gas, aerosol, and ozone changes. *Geophys. Res. Lett.*, **40**, 2302–2306, doi:10.1002/grl.50500.
- Hill, K. J., A. Santoso, and M. H. England, 2009: Interannual Tasmanian rainfall variability associated with large-scale climate modes. *J. Climate*, **22**, 4383–4397, doi:10.1175/2009JCLI2769.1.
- Hobday, A., E. Oliver, J. McDonald and M. Grose, 2016: Was Tasmania's summer of fires and floods a glimpse of its climate future. *The Conversation*, 19 April 2016. [Available online at <https://theconversation.com/was-tasmanias-summer-of-fires-and-floods-a-glimpse-of-its-climate-future-58055>.]
- Hope, P., and Coauthors, 2015: Seasonal and regional signature of the projected southern Australian rainfall reduction. *Aust. Meteor. Ocean. J.*, **65**, 54–71.
- Jones, D. A., W. Wang, and R. Fawcett, 2009: High-quality spatial climate data-sets for Australia. *Aust. Meteor. Oceanogr. J.*, **58**, 233–248.
- Kalnay, E., and Coauthors, 1996: The NCEP/NCAR 40-year reanalysis project. *Bull. Amer. Meteor. Soc.*, **77**, 437–470.
- Karoly, D. J., 1989: Southern Hemisphere circulation features associated with El Niño–Southern Oscillation events. *J. Climate*, **2**, 1239–1252.
- King, A. D., G. J. van Oldenborgh, and D. J. Karoly, 2016: Climate change and El Niño increase likelihood of Indonesian heat and drought [in "Explaining Extreme Events of 2015 from a Climate Perspective"]. *Bull. Amer. Meteor. Soc.*, **97** (12), S113–S117, doi:10.1175/BAMS-D-16-0164.1. (Chapter 19 of EEE)
- Massey, N., and Coauthors, 2015: weather@home—development and validation of a very large ensemble modelling system for probabilistic event attribution. *Quart. J. Roy. Meteor. Soc.*, **141**, 1528–1545, doi:10.1002/qj.2455.
- Mo, K. C., and R. W. Higgins, 1998: The Pacific–South American modes and tropical convection during the Southern Hemisphere winter. *Mon. Wea. Rev.*, **126**, 1581–1596.
- Taylor, K. E., R. J. Stouffer, and G. A. Meehl, 2012: An overview of CMIP5 and the experiment design. *Bull. Amer. Meteor. Soc.*, **93**, 485–498, doi:10.1175/BAMS-D-11-00094.1.